Optimal System Realization in Frequency Domain

Jer-Nan Juang *and Peiman G. Maghami †
NASA Langley Research Center
Hampton, VA 23681

Abstract

Several approaches are presented to identify an experimental system model directly from frequency response data. The formulation begins with a matrix-fraction description as the model structure. Frequency weighting such as exponential weighting is introduced to solve a weighted least-squares problem to obtain the coefficient matrices for the matrix-fraction description. A multi-variable state-space model can then be formed using the coefficient matrices of the matrix-fraction description. An approach is introduced to fine-tune the model using nonlinear programming methods to minimize the desired cost function. The method deals with the model in the real Schur or modal form and reassigns a subset of system poles using a nonlinear optimizer. At every optimization step, the input and output influence matrices are refined through least-squares procedures. The proposed approaches are used to identify an analytical model for a NASA testbed from experimental data.

1 Introduction

One major objective of system identification is to provide mathematical models for dynamics and control analysis and designs. However, models of systems can have various forms, such as transfer functions, differential or difference equations, and state-space equations. A frequency-domain state-space identification method [1 − 5] provides a state-space model of a linear system from frequency response data.

The method called the State-Space Frequency Domain (SSFD) identification algorithm [2] can estimate Markov parameters (pulse response) from the frequency response function (FRF) without window distortion when an arbitrary frequency weighting is used to shape the estimation error. The method uses a rational matrix fraction description (the ratio of a matrix polynomial and a monic scalar polynomial denominator) to curve-fit the frequency data and compute the Markov parameters from FRF. The curve-fitting problem must be solved either by nonlinear optimization techniques or by linear approximate algorithms with several iterations. To obtain the state-space models from the Markov parameters, the Eigensystem Realization Algorithm (ERA) or its variant ERA/DC is used [5].

Frequency domain methods presented in Refs. [3, 4, 5] start with identifying a left matrix-fraction description (LMFD) of the transfer function matrix. The advantage of using the LMFD, as an intermediate model between the data and the desired final state-space model, is that from frequency response data to the LMFD is a linear least-squares problem, which is easy to solve.

*Principal Scientist, Structural Dynamics Branch, (j.juang@larc.nasa.gov)
†Senior Aerospace Engineer, Guidance and Control Branch, (p.g.maghami@larc.nasa.gov)

This method works quite well when the frequency response data are fairly accurate; however, it might yield unstable, erroneous models if the data contains too much distortion and/or error. Data distortion in the frequency domain is caused by a number of factors; limited sampling frequency, filters to remove noise, and lack of periodicity. This data distortion often causes unstable modes to be present in the identified system model. An improved method was introduced in Ref. [6] to deal with the problem when data distortion is present. The idea is to stabilize or remove the unstable modes before expanding the matrix-fraction description (MFD) into the Markov parameters (pulse responses). This approach avoids introducing unstable modes while still maintaining the frequency response close to the data.

In this paper, exponential frequency weighting [2, 7] is used to solve a weighted least-squares problem for the LMFD coefficient matrices. A multi-variable state-space model is then realized from the LMFD coefficient matrices. To improve the identified model, nonlinear programming methods [8] are used to fine-tune the model parameters. A formulation is introduced in this paper for parameter optimization. This formulation deals with system realizations in the real Schur or modal forms, and uses a subset of system poles for parameter optimization. At every optimization step, the input and output influence matrices are refined through least-squares procedures. Two additional formulations for parameter optimization have also been developed. The first formulation uses a general system realization, and utilizes nonlinear programming along with an eigenvalue assignment [9 – 11] technique to adjust a subset of system poles. The second formulation deals with system realizations in the real Schur or modal forms, and uses a subset of system poles, as well as some coefficients to adjust the columns (rows) of the input (output) influence matrix for parameter optimization. These formulations are not presented here due to space limitations, however, full details on the two approaches is provided in Ref. [12]. Experimental data from a NASA testbed with fifteen inputs and fourteen outputs are used with a total of two hundreds and ten transfer functions to demonstrate the concepts proposed in this paper.

2 Weighted Least-Squares Method

Given the system frequency response function $G(z_k)$ at the frequency point z_k, consider the left matrix-fraction

$$G(z_k) = \alpha^{-1}(z_k)\beta(z_k) \tag{1}$$

where

$$\alpha(z_k) = I_m + \alpha_1 z_k^{-1} + \cdots + \alpha_p z_k^{-p} \tag{2}$$

$$\beta(z_k) = \beta_0 + \beta_1 z_k^{-1} + \cdots + \beta_p z_k^{-p} \tag{3}$$

are matrix polynomials with I_m being an identity matrix of order m. The matrix α_i is an $m \times m$ real square matrix and each β_i is an $m \times r$ real rectangular matrix. The factorization in Eq. (1) is not unique. For convenience and simplicity, one can choose the order of both polynomials to be equal to p.

Pre-multiplying Eq. (1) by $\alpha(z_k)$ produces

$$\alpha(z_k)G(z_k) = \beta(z_k) \tag{4}$$

which can be rearranged into

$$\begin{aligned} G(z_k) &= -\alpha_1 G(z_k) z_k^{-1} - \cdots - \alpha_p G(z_k) z_k^{-p} \\ &\quad + \beta_0 + \beta_1 z_k^{-1} + \cdots + \beta_p z_k^{-p} \end{aligned} \tag{5}$$

or

$$G(z_k) = \Theta \mathcal{G}_k \tag{6}$$

where the matrix Θ, of dimension $m \times [p(m+r)+r]$, and the matrix $\mathcal{G}_k$, of dimension $[p(m+r)+r] \times r$, are defined as

$$\Theta = \left[\begin{array}{cccccccc} \alpha_1 & \cdots & \alpha_p & \beta_0 & \beta_1 & \beta_2 & \cdots & \beta_p \end{array} \right] \tag{7}$$

$$\mathcal{G}_k = \left[\begin{array}{c} G(z_k) z_k^{-1} \\ \vdots \\ G(z_k) z_k^{-p} \\ I_r \\ I_r z_k^{-1} \\ \cdots \\ I_r z_k^{-p} \end{array} \right] \tag{8}$$

Here, I_r is an $r \times r$ identity matrix. With $G(z_k)$ and z_k^{-1} known, Eq. (5) or (6) is a linear equation. Because $G(z_k)$ is known at $z_k = e^{j\frac{2\pi(k-1)}{\ell}}$ $(k = 1, \ldots, \ell)$, there are ℓ equations available.

The parameter matrix Θ in Eq. (6) is a real matrix whereas $G(z_k)$ and $\mathcal{G}_k$ are both complex matrices. Thus Eq. (6) is a complex matrix equation with a total of ℓ complex equations . Let us define

$$\tilde{G}_k = [\text{Real}(G(z_k)) \;\; \text{Imag}(G(z_k))] \qquad \text{and} \qquad \tilde{\mathcal{G}}_k = [\text{Real}(\mathcal{G}_k) \;\; \text{Imag}(\mathcal{G}_k)] \tag{9}$$

Equation (6) may be rewritten as

$$\tilde{G}_k = \Theta \tilde{\mathcal{G}}_k \tag{10}$$

Equation (10) is a real matrix equation consisting of 2ℓ linear equations for computing the parameter matrix Θ. The matrix $\tilde{G}_k$ at the frequency point k is an $m \times 2r$ matrix, whereas $\tilde{\mathcal{G}}_k$ is a $[p(m + r) + r] \times 2r$ matrix.

Often, experimental data from a completed test is available which allows all calculations to be performed at once. A batch version is presented in this section. Stacking the 2ℓ equations in Eq. (10) yields

$$\tilde{G} = \Theta \tilde{\mathcal{G}} \tag{11}$$

where

$$\begin{aligned} \tilde{G} &= \left[\begin{array}{cccc} \tilde{G}_0 & \tilde{G}_1 & \cdots & \tilde{G}_\ell \end{array} \right] \\ \tilde{\mathcal{G}} &= \left[\begin{array}{cccc} \tilde{\mathcal{G}}_0 & \tilde{\mathcal{G}}_1 & \cdots & \tilde{\mathcal{G}}_\ell \end{array} \right] \end{aligned} \tag{12}$$

To solve Eq. (11), let us first define a weighted cost function to be minimized as

$$J(\Theta, \ell) = \sum_{i=1}^{\ell} w^{\ell-i} \parallel \Theta \tilde{\mathcal{G}}_{\ell-i} - \tilde{G}_{\ell-i} \parallel_2^2 \tag{13}$$

where $0 < w \leq 1$ is a forgetting factor weighting the frequency data. The data at the lowest frequency point is given unit weight, but data that is k frequency points higher is weighted by w^k. The method is commonly called exponential forgetting. The cost function defined in Eq. (13) is motivated by the fact that accelerometers are commonly used as the measurement device in structural testing. The corresponding frequency response functions have better response levels in the high frequency range. Identifying lower frequency information in the presence of measurement noise becomes a problem. One way to solve this problem is to weight more the lower frequency region. On the other hand, displacement sensors have better response capability for the low frequency region.

For this case, the forgetting factor may be switched to weight the high frequency region more than the lower frequency region. The form of Eq. (13) is unchanged except for the index $\ell - i$ is replaced by i. The least-squares solution for Θ, from Eq. (13), is given by

$$\Theta = \tilde{G}\tilde{\mathcal{G}}_w^T[\tilde{\mathcal{G}}\tilde{\mathcal{G}}_w^T]^{-1} \tag{14}$$

where

$$\tilde{\mathcal{G}}_w = \left[\begin{array}{cccc} \tilde{\mathcal{G}}_0 & w\tilde{\mathcal{G}}_1 & \cdots & w^\ell\tilde{\mathcal{G}}_\ell \end{array} \right] \tag{15}$$

The subscript w associated with $\tilde{\mathcal{G}}_w$ indicates that the forgetting factor w is inserted into $\tilde{\mathcal{G}}$ with an appropriate power at each frequency point.

The weighting w^ℓ at the frequency point ℓ can be quite small depending on the length ℓ of the data and the choice of the forgetting factor w. Fox example, $w^\ell \approx 4.3 \times 10^{-5}$ with $\ell = 1000$ and $w = 0.99$. Unless the amplitudes of those frequencies near the highest frequency are in the order of 10^{-5}, their contribution to the identification process may become negligible. Using accelerometers, the ratio of the highest frequency to the lowest frequency can be as high as 10^3 to 10^5. For this case, the forgetting factor used in Eq. (15) is indeed a good weighting technique to perform a better low-frequency identification.

On the other hand, one may prefer to have freedom of choosing a weighting factor. A slight modification of Eq. (15) will provide such freedom, i.e.,

$$\tilde{\mathcal{G}}_w = \left[\begin{array}{cccc} \tilde{\mathcal{G}}_0 & w_1\tilde{\mathcal{G}}_1 & \cdots & w_\ell\tilde{\mathcal{G}}_\ell \end{array} \right] \tag{16}$$

The quantities $w_1, w_2, \ldots, w_\ell$, can be all independent. They may be randomly or specifically chosen. Some obvious choices include

$$w_k = e^{-10(1-k)/\ell}, \quad w_k = \frac{1}{k}, \quad w_k = \frac{1}{k^2}; \quad k = 1, 2, \ldots, \ell$$

For the case where the low frequency resolution is better than the high frequency resolution, the weighting must be reversed.

Substituting Eq. (16) in Eq. (11) and solving for the parameter Θ that minimizes the following cost function,

$$J(\Theta, \ell) = \sum_{i=1}^{\ell} w_i \parallel \Theta\tilde{\mathcal{G}}_i - \tilde{G}_i \parallel_2^2 \tag{17}$$

yields results similar to Eq. (14) except for the weighting factor.

In the next section, optimization-based approaches to further improve the least-square solution are discussed.

3 Nonlinear Optimization

Another approach to enhance the identified model is to use nonlinear programming to tune the model parameters obtained from the solution to Eq. (11). Once the solution, represented by the parameter matrix Θ, is computed using Eq. (14), a state-space realization is determined. The state-space realization can be in any canonical form such as Schur form, modal form, Jordan form, observable form, etc. A formulation is introduced in this paper for parameter optimization. This formulation deals with system realizations in the real Schur or modal forms, and uses a subset of system poles for parameter optimization. The input and output influence matrices are refined through least-squares procedures at every optimization step.

As mentioned earlier, two additional formulations for parameter optimization have also been developed. The first formulation uses a general system realization, and utilizes nonlinear programming along with an eigenvalue assignment technique to adjust a subset of system poles. The second

formulation deals with system realizations in the real Schur or modal forms, and uses a subset of system poles, as well as some coefficients to adjust the columns (rows) of the input (output) influence matrix for parameter optimization. These formulations are not presented here due to space limitations, however, full details on the two approaches is provided in Ref. [12].

The details of the proposed parameter optimization approach for least-squares solution refinement is presented next. This method starts with selecting a subset of system poles as optimization parameters to minimize the error between the experimental and the identified transfer functions over a frequency range of interest. The optimizer reassigns the system poles, which reside on the diagonal elements or 2×2 block diagonal partitions of the state matrix. At each optimization step, corrections are made to the input matrix B, the output matrix C, and the direct transmission matrix D, through two least-squares solutions.

An optimization problem is presented below for improving the match between identified and experimental transfer functions. Let (A, B_0, C_0, D_0) represent an initial realization for the identified system, and parameterize the input and output influence matrices as follows,

$$B = B_0 S_b + N_{B_0} R_B = [\, B_0 \quad N_B \,] \begin{pmatrix} S_B \\ R_B \end{pmatrix} \equiv \overline{B} Q_B \tag{18}$$

$$C = S_C C_0 + R_C N_{C_0} = (\, S_C \quad R_C \,) \begin{bmatrix} C_0 \\ N_{C_0} \end{bmatrix} \equiv Q_C \overline{C} \tag{19}$$

where the columns of N_{B_0} represent a set of basis vectors in the null space of B_0, the rows of N_{C_0} represent a set of basis vectors in the null space of C_0, and Q_B, defined in terms of S_B and R_B, and Q_C, defined in terms of S_C and R_C, are the appropriate coefficient matrices. These coefficients are determined, at each optimization step, by solving least-squares-based corrections of the absolute error norm. The optimization problem is given as:

Minimize J_1*:*

$$J_1 = ||G(z_k) - \widehat{G}(z_k)||_F \tag{20}$$

over

$$\text{blkdiag}(A)$$

subject to

$$|\lambda(\text{blkdiag}(A))| < 1$$

The complex matrix $\widehat{G}(z_k)$ represents a system realization given by

$$\widehat{G}(z_k) = C(z_k I_n - A)^{-1} B + D \tag{21}$$

The constraint on the modulus of $\lambda(\text{blkdiag}(A))$ guarantees the stability of the identified system, and can be omitted if stability is not of concern. At each optimization step, as a new state matrix A is defined, corrections are performed to the B and D matrices via a least-squares solution, followed by corrections to the C and D matrices. These solutions are defined as follows.

First, let $\overline{G}(z_k) = G(z_k) - D$, and repartition the $n_d \times (m \times r)$ transfer function matrix, $\overline{G}(z_k)$, columnwise, such that each column of the repartitioned $(n_d \times m) \times r$ matrix, $\overline{G}_{col}$, is associated with an input. Define $\widehat{\overline{G}}(z_k) = C_0(z_k I_n - A)^{-1}\overline{B}$, repartition $\widehat{\overline{G}}(z_k)$ similar to $\overline{G}_{col}$ to obtain $\widehat{\overline{G}}_{col}$, and define the absolute error function as

$$e = \overline{G}_{col} - \widehat{\overline{G}}_{col} Q_B \tag{22}$$

Now, solve for Q_B, in a least-squares sense, to obtain

$$Q_B = (\widehat{\overline{G}}_{col}^T \widehat{\overline{G}}_{col})^{-1} \widehat{\overline{G}}_{col}^T \overline{G}_{col} \tag{23}$$

Once, Q_B is computed, then D is computed as

$$D = \mu\left(G(z_k) - C_0(z_k I_n - A)^{-1}B\right) \tag{24}$$

where $\mu(\ )$ denotes the mean over frequency points.

To compute Q_C, first define $\overline{G}(z_k) = G(z_k) - D$, and repartition the $n_d \times (m \times r)$ transfer function matrix, $\overline{G}(z_k)$, rowwise, such that each row of the repartitioned $m \times (n_d \times r)$ matrix, $\overline{G}_{row}$, is associated with an output. Define $\widehat{\overline{G}}(z_k) = \overline{C}(z_k I_n - A)^{-1}B$, repartition $\widehat{\overline{G}}(z_k)$ similar to $\overline{G}_{row}$ to obtain $\widehat{\overline{G}}_{row}$, and define the error function as

$$e = \overline{G}_{row} - Q_C \widehat{\overline{G}}_{row} \tag{25}$$

Now, solve for Q_C, in a least-squares sense, to obtain

$$Q_C = \overline{G}_{row}\widehat{\overline{G}}_{row}^T(\widehat{\overline{G}}_{row}\widehat{\overline{G}}_{row}^T)^{-1} \tag{26}$$

Once, Q_C is computed, then D is recomputed as

$$D = \mu\left(G(z_k) - C(z_k I_n - A)^{-1}B\right) \tag{27}$$

The number of poles that can be used as design parameters in the optimization is arbitrary. One can use all the poles in the system, or just a few, for example, the real poles of the system. If one starts the optimization with a system realization from the least-squares solution of Eq. (14), then it is very likely that the complex poles of the identified system, representing resonant peaks in the frequency response plots, match the experimental results well, and hence need not be manipulated any further. In such a case, real poles of the system and unstable poles, real or complex, are the best candidates for design optimization. However, one could conceivably use the modulus of all complex poles, which determine the damping associated with each mode, as design parameters as well.

One of the problems with nonlinear programming is the tendency of the solution to converge to a local minimum. The problem becomes more aggravated as the number of design parameters increases. One way to deal with this problem is to restart the optimization from another set of design points in the neighborhood of the last optimal design. Another way of avoiding this problem is to introduce an additional constraint requiring that the cost function be less than a desired value, i.e.,

$$J \leq J_d \tag{28}$$

This constraint would move many of the local minima to the infeasible region, thereby avoiding them.

The cost function in Eq. (20), which is the Frobenius norm of the error in the transfer functions (experimental and identified), is dominated by the peaks (resonants) of the transfer functions. Hence, optimization with Eq. (20) works well in reducing the errors at or around those peaks, or wherever the transfer function magnitude is significant, but it may not do much in reducing the errors elsewhere, e.g., zeros. In fact, the errors around the valleys might become worst. A more equitable trade between the errors for peaks and valleys can be obtained by considering a complementary optimization problem, wherein a norm of the relative error is optimized instead of the absolute error given in Eq. (20). Details of this optimization problem are provided in Ref. [12].

4 Applications

This section describes the application of the proposed techniques to the system identification for the PARTI wind-tunnel model [13], a laboratory test structure at NASA Langley. The model is

a five-foot long, high aspect ratio wing designed to flutter at low speeds to simplify aerodynamic analyses and wind-tunnel testing. The fully assembled semi-span model is shown in Fig. 1. The model has a total of 72 actuators bonded to both sides of the plate. Each actuator contains two stacks of two 0.01 inch piezoelectric patches. The 72 actuators are hardwired to actuate in 15 different groups. The 15 groupings were chosen such that each group primarily affects one of the first three natural modes. Each group can be considered as one input, because all the actuators in the group use the same signal. The piezoelectric patches were only used for actuation; ten strain gages and four accelerometers were used as sensors. As a result, there are a total of 15 inputs and 14 outputs. Due to space limitations, only a few of the results are presented here. A full presentation and discussion of the results are given in Ref. [12].

4.1 Weighted Least-Squares Solution

In the first application, the transfer function from input No. 1 to all outputs is considered for identification. With signals from 14 sensor outputs ($m = 14$), input No. 1 ($r = 1$), and 10th order polynomials ($p = 10$) used in the matrix-fraction expansion (see Eqs. (1)-(3)), a weighted least-squares solution was first obtained from Eq. (14), using an exponential weighting function, given as

$$w^k \; ; \quad k = 0, 1, \ldots, \ell$$

Here, $k = 0$ refers to the zero frequency component of the FRF often known as the direct current (DC) term in electrical engineering, and w was chosen at 0.98. By adjusting the value of w one may emphasize the low frequencies or the higher frequencies. Values of w less than 1 would emphasize the lower end of the frequency spectrum. Here, w was set to 0.98, to emphasize the range of frequency from 0 to 25 Hz. The weighted least-squares solution resulted in an identified model of order 140, which included 4 unstable poles. However, since the actual testbed is stable, it is desired to obtain a stable identified model. Truncating the unstable states yielded a 136-order state-space realization of the system. Magnitude and phase FRF plots for output No. 7 are shown in Fig.2.

Comparison of the plots indicates an excellent agreement between the experimental FRF (solid line) and the identified FRF (dashed line), particularly around the peaks of the FRF or where the gain values are significant. However, discrepancies can be observed around some of the zeros as well as where the gain values are small. This should be expected because the least-squares problem is dominated by the peaks and large gain values. Further inspection of these plots also indicates that the agreement between the experimental and identified results is better in the 0-25 Hz range. The Frobenius norm of the error between the experimental and identified transfer functions was computed at 90.128, the majority of which is due to the differences between two FRFs at DC frequency. In fact, since the DC gain values are quite large, particularly in some output channels, they tend to dominate the rest of the FRF in a least-squares solution. Keep in mind that the DC gain values may not be accurate due to the use of accelerometers and their insensitivity at very low frequencies, drift problems that hampers accurate measurements, and lack of sufficient data. Therefore, in this case, it is reasonable to de-emphasize the DC values by assigning a zero value to the corresponding weighting function, such that the DC weight is set to zero. The FRF plots, using the *modified weighting function*, are shown in Fig. 2 as dashed-dotted lines. This figure indicates moderate improvements in various frequency ranges. The Frobenius norm of the error between the experimental and identified transfer functions was computed to be 90.134, a very minor change from the previous results. Comparing, the norm of the error for all frequency points except DC, shows that the error went down from 0.241 to 0.223, which quantifies the better match by using the modified weighting function. In order to show the effectiveness of the modified exponential weighting, a polynomial with $p = 3$ is used in the matrix-fraction description. The weighted least-squares solution resulted in a stable identified model of order 40. Figure 3 illustrate the stable least-squares solutions for the nominal and modified exponential weightings for output No. 7. These figures clearly demonstrate the advantage of modified exponential weighting for this problem. In fact, the Frobenius norm of the error between the experimental and identified transfer functions dropped from 12.035 to 0.3021, a significant improvement.

4.2 Further Enhancements: Nonlinear Programming

To demonstrate the potential of the nonlinear programming approaches to further enhance the least-squares solution, the parameter optimization approach, posed in Eq. (20), is applied to an identified model for the PARTI testbed, obtained from a least-squares solution. In this optimization, the Frobenius norm of the absolute error is minimized while adjusting the eigenvalues of the state matrix, subject to stability constraints. Moreover, the optimization included corrections to the B and D matrices, followed by corrections to the C and D matrices, at each functional evaluation (see Eq. (23)-(24) and (26)-(27)). The 6 design variables used in the optimization were the values of the real poles of the system. The optimization included 7 constraints, the first six to guarantee the stability of the systems as the poles were reassigned, and a constraint on the value of the error norm to avoid undesirable local minima. The initial design used in the optimization was taken from a stable least-squares solution with modified exponential weighting, i.e., zero DC weighting. The optimization reduced the norm of the absolute error from the initial value of 0.250 to 0.197, which is over 20% reduction. Plots, comparing the FRF matrices for the experimental, nominal, and optimal results are provided in Fig. 4, for output No. 7. The identified model (via optimization) agrees very well with the experimental data.

All the identification results obtained so far were based on the 14 FRFs from the first input to all 14 outputs. Now, let us consider the FRFs from all 15 inputs to all 14 outputs for identification. With the signals from all 14 sensor outputs ($m = 14$) and all 15 inputs ($r = 15$), and 3rd order polynomials ($p = 3$) used in the matrix-fraction expansion(see Eqs. (1)-(3)), a weighted least square solution was first obtained from Eq. (14). Similar to the previous cases, an exponential weighting function was used, with parameter w chosen at 0.98 to emphasize the range of low frequencies. In addition, the DC weight was set to zero. The Frobenius norm of the error between the experimental and identified FRFs was computed at 246.855, the majority of which is due to a discrepancy between two FRFs at the DC frequency, i.e., zero frequency. The Frobenius norm of the absolute error, for all frequency points except the DC, was computed to be 1.721. For the purpose of illustration, plots for the experimental and realized FRFs are depicted in Fig. 5, for output No. 7 with input No. 1, and in Fig.6, for the same output with input No. 8. The experimental transfer functions are shown as solid lines and the transfer functions, obtained via direct least square, as dashed lines. These figures indicate moderate to good agreement between the transfer functions in low frequencies ranges, particularly, around the peaks or high gain areas of the transfer functions.

Now consider the least-squares optimization approach presented in Eq. (20) for the 15 inputs and 14 output case. The initial design used in the optimization was the stable least-squares solution with modified exponential weighting. This realization had 14 real poles, whose locations were used as design variables in the optimization, i.e., there were 14 design variables. The optimization included 15 constraints, the first 14 to guarantee the stability of the systems as the poles were reassigned, and the last constraint on the value of the error norm to avoid convergence to undesirable local minima. The optimization reduced the norm of the error from the initial value of 1.165 to 1.090, about a 6.5% reduction. Plots, comparing for the experimental (solid line), nominal (dashed line), and optimal transfer function (dashed-dotted line) are provided in Figs. 5 and 6. It is observed that the identified model (obtained via optimization) performs well, although only 3rd order polynomials were used in the matrix fraction description to match a 15 input by 14 output transfer function. Comparing Fig. 5 and Fig. 4, which correspond to the same input and output channels, confirms the good level of correlation obtained following the optimization-based approach.

5 Concluding Remarks

Several techniques have been presented to identify an experimental system model directly from frequency response data. The techniques used a matrix-fraction description (MFD) to describe the identified system. The MFD coefficients were obtained from the solution of a weighted least-squares problem. Frequency weighting concepts were introduced in order to emphasize a frequency range of interest. An optimization-based method was introduced to fine-tune the experimentally realized

models. The method adjusts a subset of the system poles to improve the identified model. The input and output influence matrices are computed at every optimization step through least-squares procedure. These techniques were applied to data from PARTI wind tunnel model, a laboratory testbed at NASA Langley Research Center. The benefits of the optimization-based refinement technique as well as frequency weighting techniques were demonstrated. It was shown that with optimal fine-tuning and proper choice of frequency weighting a 40th order system realization could provide almost the same level of model fit as a full-order 136th order model. The numerical computation of the gradients may require a large number of functional evaluation, which would be costly in a computational sense. Alternatively, one may attempt to obtain analytical expressions for the gradients, and perhaps second-order partial derivatives, to improve computational efficiency and accuracy.

References

[1] Juang, J.-N. and Suzuki, H., "An Eigensystem Realization in Frequency Domain for Modal Parameter Identification," *Journal of Vibration, Acoustics, Stress and Reliability in Design,* Vol. 110, No. 1, January 1988, pp. 24-29.

[2] Bayard, D. S., "An Algorithm for State Space Frequency Domain Identification without Windowing Distortions," *Proceedings of the Control and Decision Conference*, December 1992.

[3] Chen, C. W., Juang, J.-N., and Lee, G., "Frequency Domain State-Space System Identification," *Transactions of the ASME, Journal of Vibration and Acoustics*, Vol. 116, No. 4, Oct. 1994, pp. 523-528

[4] Horta, L. G., Juang, J.-N., and Chen, C.-W., "Frequency Domain Identification Toolbox," *NASA Technical Memorandum 109039*, September 1996, pp. 1-28.

[5] Juang, J.-N., *Applied System Identification*, Prentice Hall, Inc., Englewood Cliffs, New Jersey 07632, 1994, ISBN 0-13-079211-X.

[6] Chen, C.-W., Juang, J.-N., and Lee, G., "Stable State Space System Identification from Frequency Domain Data," *Proceedings of the first IEEE Regional Conference on Aerospace Control Systems*, CA., May 25-27, 1993.

[7] Astrom, K.J., and Witenmark, B., *Adaptive Control,* Addison-Wesley Publishing Company, 1995.

[8] Gill, P. E., Murray, W., and Wright, M. H., *Practical Optimization*, John Academic Press, London, 1981.

[9] Juang, J. N., Lim, K. B., and Junkins, J. L., "Robust Eigensystem Assignment for Flexible Structures," *Journal of Guidance, Control and Dynamics,* Vol. 12, No. 3, May-June 1989, pp. 381-387.

[10] Maghami, P. G., and Juang, J. N., "Efficient Eigenvalue Assignment for Large Space Structures," *Journal of Guidance, Control and Dynamics,* Vol. 13, No. 6, Nov.-Dec. 1990, pp. 1033-1039.

[11] Juang, J. N., and Maghami, P. G., "Robust Eigensystem Assignment for Second Order Dynamics System," *Mechanics and Control of Large Space Structures* edited by John L. Junkins, AIAA Monograph on Progress in Astronautics and Aeronautics, Vol 29, 1990, pp. 373-387.

[12] Juang, J. N., and Maghami, P., "Optimal Frequency-Domain System Realization with Weighting" to be published as *NASA TM,* 1999.

[13] McGowan, A. R., Heeg, J., and Lake, R. C., "Results of Wind-Tunnel Testing from the Piezoelectric Aeroelastic Response Tailoring Investigation," 1996 Structures, Structural Dynamics, and Materials Conference.

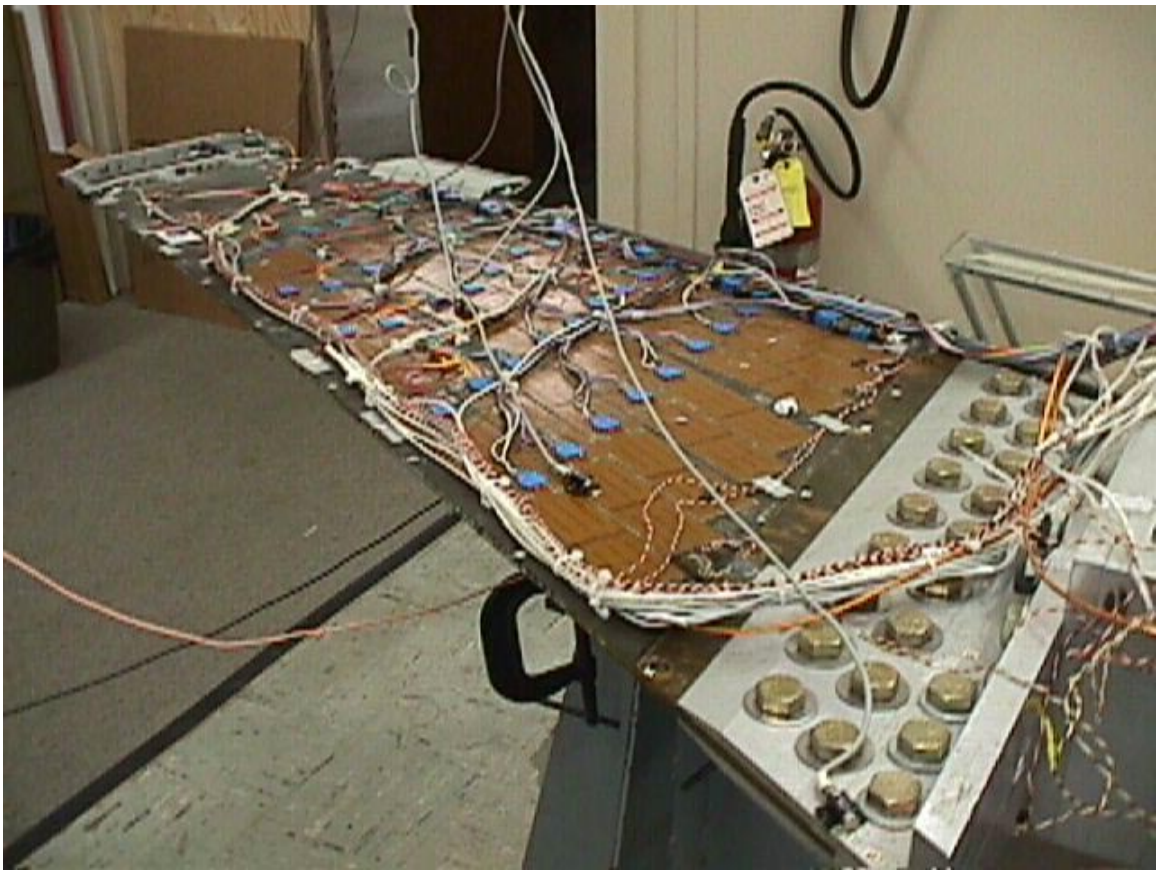

Figure 1: PARTI Model

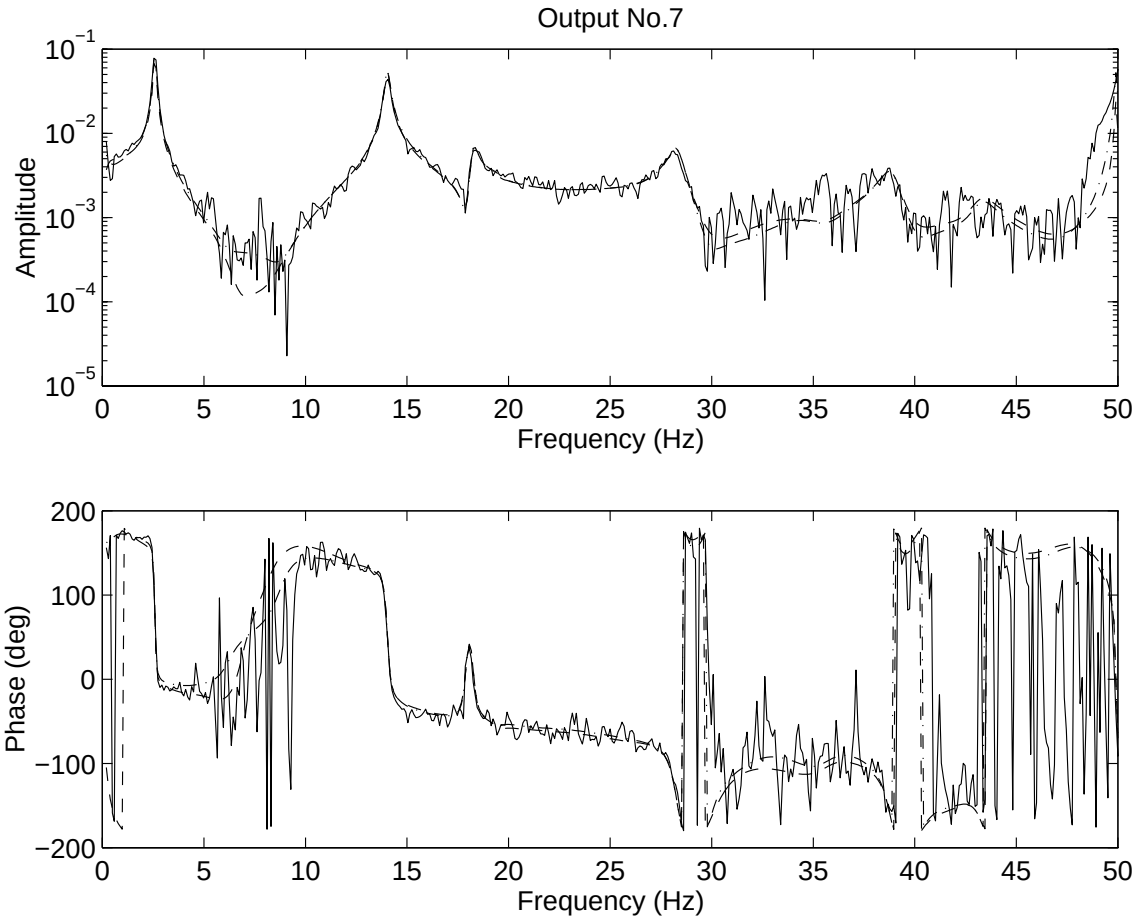

Figure 2: Comparison of FRFs for Output No. 7 with exponential weighting and 136-order system: experimental FRF (solid line), identified FRF (dashed line), identified FRF with zero DC weighting (dashed-dotted line).

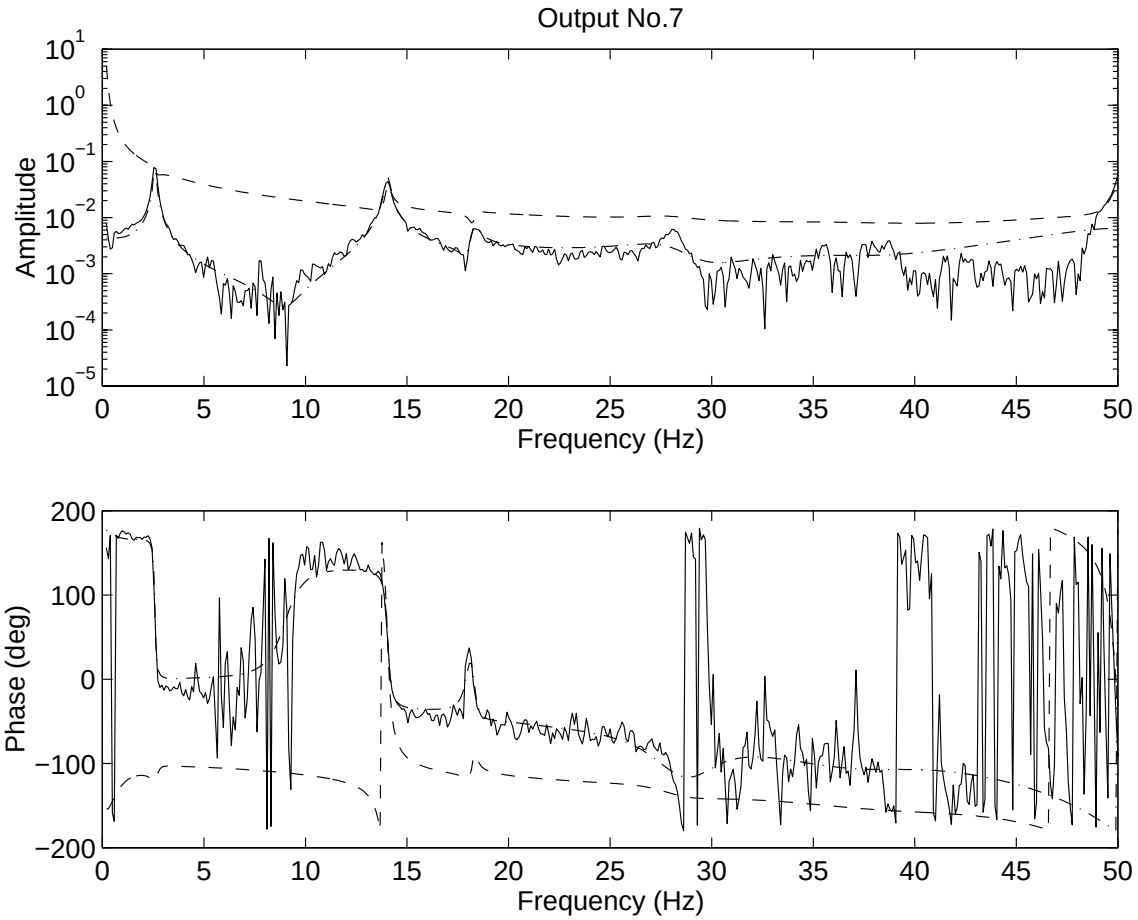

Figure 3: Comparison of FRFs for Output No. 7 with exponential weighting and 40-order of system: experimental FRF (solid line), identified FRF (dashed line), identified FRF with zero DC weighting (dashed-dotted line)

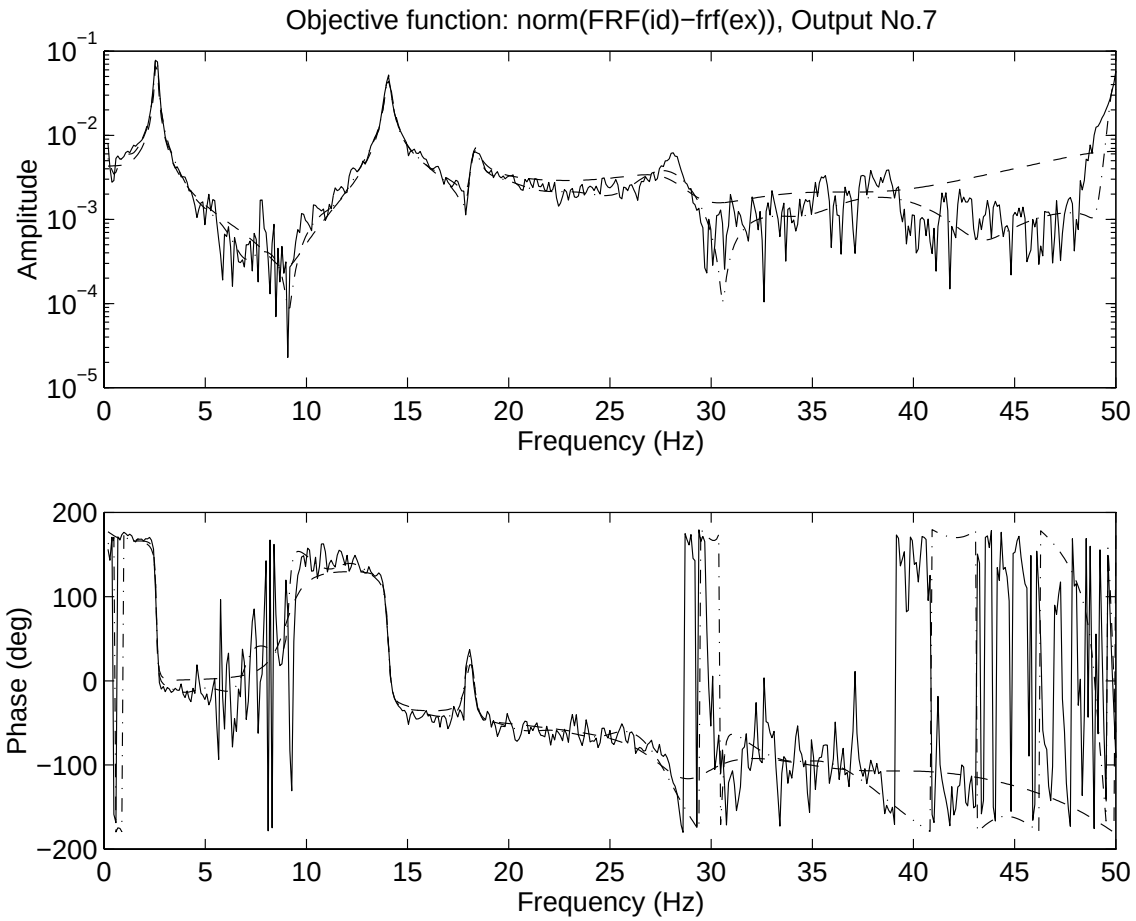

Figure 4: Comparison of FRFs for Output No. 7 with least-squares optimization approach and 40-order system: experimental FRF (solid line), identified FRF (dashed line) with zero DC weighting, enhanced FRF with absolute-error optimization (dashed-dotted line)

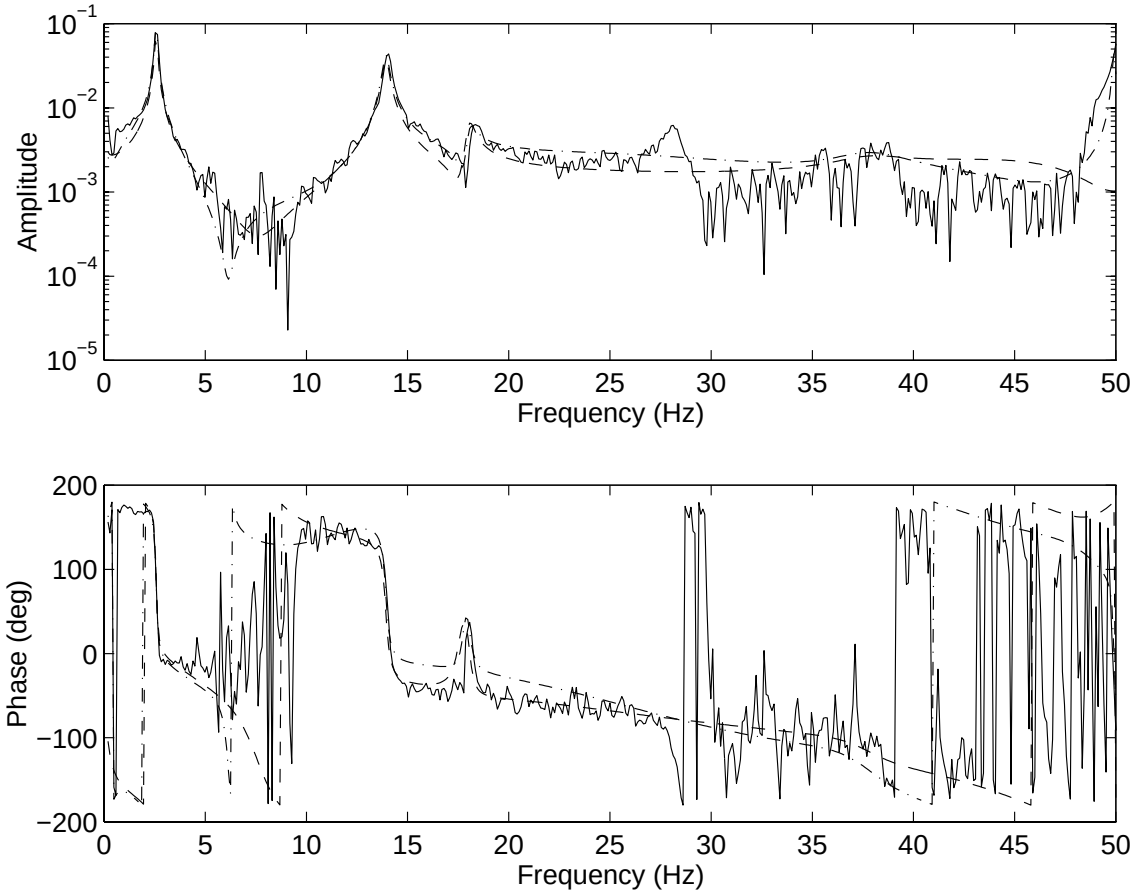

Figure 5: Comparison of FRFs for Output No. 7 and Input No. 1 with least-squares optimization approach and 42-order system: experimental FRF (solid line), identified FRF (dashed line) with zero DC weighting, enhanced FRF with absolute-error optimization (dashed-dotted line)

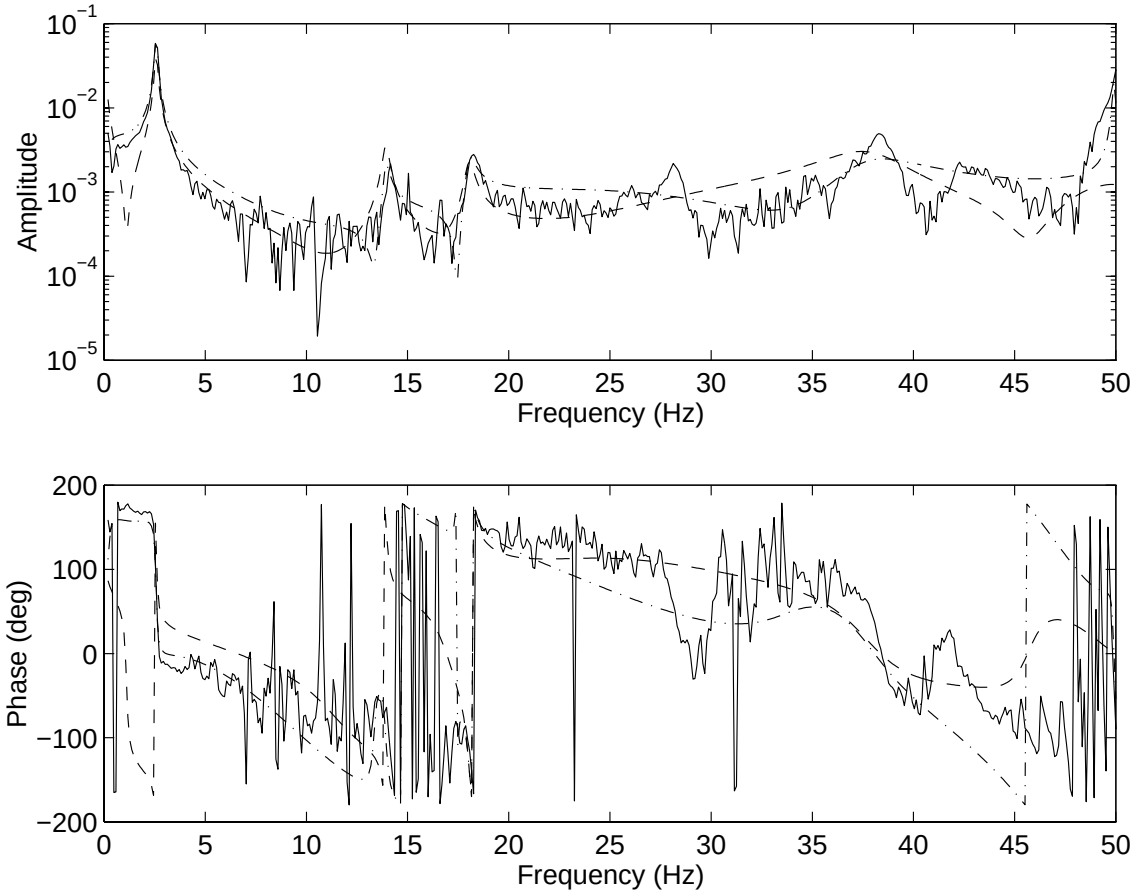

Figure 6: Comparison of FRFs for Output No. 7 and Input No. 8 with least-squares optimization approach and 42-order system: experimental FRF (solid line), identified FRF (dashed line) with zero DC weighting, enhanced FRF with absolute-error optimization (dashed-dotted line)